Contemporary Mathematics
https://ojs.wiserpub.com/index.php/CM/

Research Article

Cnoidal Waves, Solitary Waves, Shock Waves and Conservation Laws of the Generalized Cubic Boussinesq-Type Model for Shallow Water Wave Dynamics

Anjan Biswas[1,2,3,4], Ming-Yue Wang[5], Abdul H. Kara[6], Yakup Yildirim[7,8*], Luminita Moraru[9,10], Carmelia M. Balanica[3], Layth Hussein[11,12,13], Anwar Ja'far Mohamad Jawad[14]

[1]Department of Mathematics and Physics, Grambling State University, Grambling, LA, 71245-2715, USA
[2]Department of Physics and Electronics, Khazar University, Baku, AZ, 1096, Azerbaijan
[3]Department of Applied Sciences, Cross-Border Faculty of Humanities, Economics and Engineering, Dunarea de Jos University of Galati, 111 Domneasca Street, Galati, 800201, Romania
[4]Department of Mathematics and Applied Mathematics, Sefako Makgatho Health Sciences University, Medunsa, 0204, South Africa
[5]Key Laboratory of Mechanics on Disaster and Environment in Western China, The Ministry of Education, College of Civil Engineering and Mechanics, Lanzhou University, Lanzhou, 730000, China
[6]School of Mathematics, University of the Witwatersrand, Private Bag 3, Wits, 2050, Johannesburg, South Africa
[7]Department of Computer Engineering, Biruni University, Istanbul, 34010, Turkey
[8]Mathematics Research Center, Near East University, 99138, Nicosia, Cyprus
[9]Department of Chemistry, Physics and Environment, Faculty of Sciences and Environment, Dunarea de Jos University of Galati, 47 Domneasca Street, 800008, Romania
[10]Department of Physics, School of Science and Technology, Sefako Makgatho Health Sciences University, Medunsa, 0204, Pretoria, South Africa
[11]Department of Computers Techniques Engineering, College of Technical Engineering, The Islamic University, Najaf, Iraq
[12]Department of Computers Technique Engineering, College of Technical Engineering, The Islamic University of Al Diwaniyah, Al Diwaniyah, Iraq
[13]Department of Computers Techniques Engineering, College of Technical Engineering, The Islamic University of Babylon, Babylon, Iraq
[14]Department of Computer Technical Engineering, Al-Rafidain University College, Baghdad, 10064, Iraq
E-mail: yyildirim@biruni.edu.tr

Received: 10 January 2025; **Revised:** 22 February 2025; **Accepted:** 12 March 2025

Abstract: The paper addresses the latest form of Boussinesq equation with generalized form of cubic nonlinearity. The solitary waves are recovered from the model using traveling wave hypothesis. The conservation laws are recovered from the model. The conservation laws are obtained using the method of multipliers. Finally, the complete discriminant method yields shock waves and cnoidal waves as well. The numerical simulations supplement the analytical results.

***Keywords*:** solitary waves, shallow water, Boussinesq, conservation laws

MSC: 35C08, 76B25

DOI: https://doi.org/10.37256/cm.6220256389

1. Introduction

The theory of shallow water waves flow is one of the most longest existing areas of study in Fluid Dynamics [1–5]. Starting from the well-known model, namely the Euler's equation, several models have emerged with low depth approximation [6–8]. The most common is the Korteweg-de Vries equation in one spatial dimensions that was later extended to two spatial dimensions and is known as Kadomtsev-Petviashvili equation [9–11]. There are several other equations to model shallow water wave dynamics emerged [12]. They are the Kawahara equation and later the Boussinesq equation. This Boussinesq equation was recently addressed with the inclusion of surface tension effect [2]. This model with surface tension included the effect of sixth-order dispersion and the model has been studied to recover a few of the preliminary results. The solitary waves, shock waves and the singular solitary waves were recovered. The conservation laws were also identified. The results have been recently reported during 2023.

The current paper takes up a recently proposed a newly structured Boussinesq equation that was proposed during 2023 [1]. This model is addressed in the paper with generalized form of cubic nonlinearity. The traveling wave hypothesis recovered the solitary wave solutions. The corresponding conservation laws were also retrieved by the method of multipliers and classified. Subsequently, the cubic version of this model is analyzed using the complete discriminant method. This gave way to several additional forms of solutions such as singular solitary waves, shock waves, cnoidal waves and plane waves. Additionally, a byproduct of this approach yielded singular periodic solutions and periodic solutions. The results are all exhibited and inked in details.

1.1 *Governing model*

The lately proposed generalized cubic Boussinesq-type model is structured with generalized cubic form of nonlinearity, as [1]:

$$q_{tt} - k^2 q_{xx} + a q_{xt} + b q_{xxxx} + c q_{xxxt} + d q_{xxtt} + \alpha \left(q^{2n+1}\right)_{xx} = 0. \tag{1}$$

Here, in (1), $q(x,\, t)$ represents the wave amplitude while the independent variables t and x are the temporal and spatial variables. The spatio-temporal dispersion is the coefficient of a while the fourth-order dispersion effects are given by the coefficients of $b,\ c$ and d. Finally, the nonlinear effect comes from the coefficient of α. The full nonlinearity parameter n gives the model a generalized flavor. This model has been studied for $n = 1$ where solitary waves and two-component nonlinear waves have been recovered [1].

2. Solitary waves

The solitary wave reads as

$$q(x,\, t) = g(x - vt). \tag{2}$$

Substituting (2) into (1) gives the ordinary differential equation (ODE)

$$\left(v^2 - k^2 - av\right) g'' + \left(b - cv + dv^2\right) g^{(iv)} + \alpha \left(g^{2n+1}\right)'' = 0. \tag{3}$$

Integrating (3) and setting the integration constants to be zero, leads to

$$\left(v^2-k^2-av\right)g-\left(cv-dv^2-b\right)g''+\alpha g^{2n+1}=0. \tag{4}$$

Next multiplying by g' and integrating while taking the integration constant to be zero gives

$$\left(v^2-k^2-av\right)g^2-\left(cv-dv^2-b\right)\left(g'\right)^2+\frac{\alpha}{n+1}g^{2n+1}=0, \tag{5}$$

which when integrated gives the solution

$$q(x,\,t)=g(x-vt)=A\,\mathrm{sech}^{\frac{1}{n}}\left[B(x-vt)\right], \tag{6}$$

here the inverse width B and the amplitude A of the solitary wave are given as:

$$A=\left[-\frac{(n+1)\left(v^2-k^2-av\right)}{\alpha}\right]^{\frac{1}{2n}}, \tag{7}$$

and

$$B=n\sqrt{\frac{v^2-k^2-av}{cv-dv^2-b}}. \tag{8}$$

These introduce the parameter constraints:

$$\alpha\left(v^2-k^2-av\right)<0, \tag{9}$$

and

$$\left(v^2-k^2-av\right)\left(cv-dv^2-b\right)>0, \tag{10}$$

for the solitary waves to exist.

3. Conservation laws

For nonlinear evolution equations of n independent variables $\mathbf{x}$ and dependent variables $\mathbf{u}$

$$G^{\mu}\left(\mathbf{x},\,\mathbf{u},\,u_{(1)},\,\ldots,\,u_{(r)}\right)=0,\;\mu=1,\,\ldots,\,\tilde{m}, \tag{11}$$

where $u_{(1)}, u_{(2)}, \ldots, u_{(r)}$ denote the collections of all first, second, …, order partial derivatives. A vector $T = (T^1, \ldots, T^n)$ is conserved if it satisfies the divergence

$$D_i T^i = 0 \tag{12}$$

along the solutions of (11). It can be shown that every admitted conservation law arises from *multipliers* $Q^\mu(\mathbf{x}, \mathbf{u}, u_{(1)}, \ldots)$ such that

$$Q^\mu G^\mu = D_i T^i \tag{13}$$

holds identically (i.e., off the solution space). The conserved flow T is then obtained by a well known 'homotopy' formula. For (1), we obtain the multipliers Q^j with corresponding conserved flows $T_j = (T_j^t, T_j^x)$, for $j = 1, \ldots, 4$.

$Q^1 = 1$:

$$\begin{aligned} T_1^t &= \frac{dq_{xxt}}{2} + \frac{cq_{xxx}}{4} + q_t + \frac{aq_x}{2}, \\ T_1^x &= 8\alpha n q_x q^{2n+1} - 4k^2 q_x q + 4\alpha q_x q^{2n+1} + 2aq_t q + 4bq_{xxx} q + 3cq_{xxt} q + 2dq_{xtt} q. \end{aligned} \tag{14}$$

$Q^2 = t$:

$$\begin{aligned} T_2^t &= \frac{1}{2} t d q_{xxt} + \frac{1}{4} t c q_{xxx} - \frac{1}{6} d q_{xx} + t q_t + \frac{1}{2} t a q_x - q, \\ T_2^x &= \frac{1}{12q} \big[24 t \alpha n q_x q^{2n+1} - 12 k^2 t q_x q + 12 \alpha t q_x q^{2n+1} + 6 t a q_t q + 12 t b q_{xxx} q + 9 t c q_{xxt} q \\ &\quad + 6 t d q_{xtt} q - 6 a q^2 - 3 c q_{xx} q - 4 d q_{xt} q \big]. \end{aligned} \tag{15}$$

$Q^3 = x$:

$$\begin{aligned} T_3^t &= \frac{1}{2} x d q_{xxt} + \frac{1}{4} x c q_{xxx} - \frac{1}{3} d q_{xt} - \frac{1}{4} c q_{xx} + x q_t + \frac{1}{2} x a q_x - \frac{1}{2} a q, \\ T_3^x &= -\frac{1}{12q} \big[-24 \alpha n x q_x q^{2n+1} + 12 x k^2 q_x q - 12 \alpha x q_x q^{2n+1} - 6 x a q_t q - 12 x b q_{xxx} q - 9 x c q_{xxt} q \\ &\quad - 6 x d q_{xtt} q - 12 k^2 q^2 + 12 b q_{xx} q + 6 c q_{xt} q + 2 d q_{tt} q + 12 \alpha q^{2n+2} \big]. \end{aligned} \tag{16}$$

$Q^4 = \frac{1}{2}t^2 - \frac{1}{a}xt$:

$$T_4^t = \frac{1}{24a}\left[6a^2t^2q_x + 3act^2q_{xxx} + 6adt^2q_{xxt} - 4adtq_{xx} + 12at^2q_t\right.$$

$$- 12atxq_x - 6ctxq_{xxx} - 12dtxq_{xxt} - 12atq + 6ctq_{xx} + 8dtq_{xt} + 4dxq_{xx} - 24txq_t - 8dq_x + 24q_x\Big],$$

$$T_4^x = -\frac{1}{24aq}\left[-4tdq_{tt}q - 8dxq_{xt}q - 12ctq_{xt}q - 6cxq_{xx}q - 24btq_{xx}q - 4adq_xq - 6a^2t^2q_tq\right.$$

$$- 24a\alpha nt^2q_xq^{2n+1} + 48\alpha ntxq_xq^{2n+1} - 6adt^2q_{xtt}q + 8adtq_{xt}q + 6actq_{xx}q - 9act^2q_{xxt}q$$

$$- 12abt^2q_{xxx}q + 12dtxq_{xtt}q - 24k^2txq_xq + 12atxq_tq + 24btxq_{xxx}q + 18ctxq_{xxt}q$$

$$+ 12ak^2t^2q_xq - 12a\alpha t^2q_xq^{2n+1} + 24\alpha txq_xq^{2n+1} - 24\alpha tq^{2n+2} + 12a^2tq^2 - 12axq^2$$

$$\left.+ 24k^2tq^2 + 12cq_xq + 8dq_tq\right]. \tag{17}$$

The T_j^t are the conserved densities in each case.
The corresponding conserved quantities are:

$$I_1 = \int_{-\infty}^{\infty} T_1^t dx = 0, \tag{18}$$

$$I_2 = \int_{-\infty}^{\infty} T_2^t dx = \frac{A}{B}\frac{\Gamma\left(\frac{1}{2n}\right)\Gamma\left(\frac{1}{2}\right)}{\Gamma\left(\frac{1}{2n}+\frac{1}{2}\right)}, \tag{19}$$

$$I_3 = \int_{-\infty}^{\infty} T_3^t dx = \frac{(v-a)A}{B}\frac{\Gamma\left(\frac{1}{2n}\right)\Gamma\left(\frac{1}{2}\right)}{\Gamma\left(\frac{1}{2n}+\frac{1}{2}\right)}, \tag{20}$$

and

$$I_4 = \int_{-\infty}^{\infty} T_4^t dx = -\frac{vtA}{aB}\frac{\Gamma\left(\frac{1}{2n}\right)\Gamma\left(\frac{1}{2}\right)}{\Gamma\left(\frac{1}{2n}+\frac{1}{2}\right)}. \tag{21}$$

Thus, I_4 will be a conserved quantity provided $dT_4^t/dt = 0$ which would imply

$$v = 0. \tag{22}$$

This means that I_4 would be a conserved quantity for stationary solitary waves only-an interesting observation.

4. Complete discriminant approach

The special case of the given model (1) with $n = 1$ will be now addressed. For $n = 1$, the model given by (1) restructures to:

$$q_{tt} - k^2 q_{xx} + a q_{xt} + b q_{xxxx} + c q_{xxxt} + d q_{xxtt} + \alpha q_{xx}^3 = 0. \tag{23}$$

To start off, the starting hypothesis selected to be:

$$q = q(\xi),\ \xi = x - vt. \tag{24}$$

Inserting (2) into (1) gives the ODE:

$$\left(v^2 - k^2 - av\right) q'' + \left(b - cv + dv^2\right) q^{(iv)} + \alpha \left(q^3\right)'' = 0. \tag{25}$$

Integrating (25) and setting the integration constants to be e_0, leads to

$$\left(v^2 - k^2 - av\right) q - \left(cv - dv^2 - b\right) q'' + \alpha q^3 + e_0 = 0. \tag{26}$$

Next multiplying by g' and integrating while taking the integration constant to be e_1 gives

$$\left(v^2 - k^2 - av\right) q^2 - \left(cv - dv^2 - b\right) \left(q'\right)^2 + \frac{\alpha}{2} q^4 + 2e_0 q + e_1 = 0. \tag{27}$$

Simplify Eq.(27) to the integral form

$$\pm \frac{\alpha}{2(cv - dv^2 - b)} \xi - \xi_0 = \int \frac{dq}{\sqrt{F(q)}}. \tag{28}$$

Here

$$F(q) = q^4 + h_2 q^2 + h_1 q + h_0, \tag{29}$$

$$h_2 = \frac{2(v^2 - k^2 - av)}{\alpha},$$

$$h_1 = \frac{4e_0}{\alpha}, \tag{30}$$

$$h_0 = \frac{2e_1}{\alpha}.$$

We employ the approach to address the integral (28), and thus obtain the solutions of model (1).

By employing the complete discrimination system for the polynomial $F(q)$ in equation (29), defined by the following expressions [3, 4]:

$$\begin{aligned} D_1 &= 1, \\ D_2 &= -h_2, \\ D_3 &= -2h_2^3 + 8h_2h_0 - 9h_1^2, \\ D_4 &= -h_2^3h_1^2 + 4h_2^4h_0 + 36h_2h_1^2h_0 - 32h_2^2h_0^2 - \frac{27}{4}h_1^4 + 64h_0^3, \\ E_2 &= 9h_1^2 - 32h_2h_0, \end{aligned} \tag{31}$$

the roots of $F(q)$ are divided into nine distinct cases, leading to the solution of integral (28).

Case 1: $D_2 < 0,\ D_3 = D_4 = 0,\ E_2 < 0$, then $F(q) = [(q - s_1)^2 + s_2^2]^2$, a singular periodic solution comes out as

$$q_1 = s_2 \tan\left(s_2 \frac{\alpha}{2(cv - dv^2 - b)}\xi - \xi_0\right) + s_1, \tag{32}$$

where s_1 and s_2 are real constants.

Case 2: $D_2 = 0,\ D_3 = 0,\ D_4 = 0$, then $F(q) = q^4$, plane waves that emerged are

$$q_2 = -\left(\frac{\alpha}{2(cv - dv^2 - b)}\xi - \xi_0\right)^{-1}. \tag{33}$$

Case 3: $D_2 > 0,\ D_3 = D_4 = 0,\ E_2 > 0$, then $F(q) = (q - s_1)^2(q - s_2)^2$, singular solitary wave and shock wave solutions come out respectively as

$$q_3 = \frac{s_2 - s_1}{2}\left(\coth\frac{(s_1-s_2)\left[\dfrac{\alpha}{2(cv-dv^2-b)}\xi-\xi_0\right]}{2} - 1\right) + s_2, \tag{34}$$

and

$$q_4 = \frac{s_2 - s_1}{2}\left(\tanh\frac{(s_1-s_2)\left[\dfrac{\alpha}{2(cv-dv^2-b)}\xi-\xi_0\right]}{2} - 1\right) + s_2, \tag{35}$$

where s_1 and s_2 are real constants.

Case 4: $D_2 > 0,\ D_3 > 0,\ D_4 = 0$, then $F(q) = (q-s_1)^2(q-s_2)(q-s_3)$, a solitary wave solution comes out as

$$q_5 = \frac{2(s_1-s_2)(s_1-s_3)}{(s_2-s_3)\cosh\left[\sqrt{(s_1-s_2)(s_1-s_3)}\left(\dfrac{\alpha}{2(cv-dv^2-b)}\xi-\xi_0\right)\right] - (2s_1-s_2-s_3)}, \tag{36}$$

and a singular periodic solution comes out as

$$q_6 = \frac{2(s_1-s_2)(s_1-s_3)}{\pm(s_2-s_3)\sin\left[\sqrt{-(s_1-s_2)(s_1-s_3)}\left(\dfrac{\alpha}{2(cv-dv^2-b)}\xi-\xi_0\right)\right] - (2s_1-s_2-s_3)}, \tag{37}$$

where $s_1,\ s_2$ and s_3 are real constants.

Case 5: $D_2 > 0,\ D_3 = D_4 = 0,\ E_2 = 0$, then $F(q) = (q-s_1)^3(q-s_2)$, an rational singular solution comes out as

$$q_7 = s_1 + \frac{4(s_1-s_2)}{(s_2-s_1)^2\left[\dfrac{\alpha}{2(cv-dv^2-b)}\xi-\xi_0\right]^2 - 4}, \tag{38}$$

where s_1 and s_2 are real constants.

Case 6: $D_2D_3 < 0,\ D_4 = 0$, then $F(q) = (q-s_1)^2[(q-s_2)^2+s_3^2]$, an exponential solution comes out as

$$q_8 = \frac{e^{\pm\sqrt{(s_1-s_2)^2+s_3^2}\left(\frac{\alpha}{2(cv-dv^2-b)}\xi-\xi_0\right)} - \dfrac{s_1-2s_2}{\sqrt{(s_1-s_2)^2+s_3^2}} + 2\sqrt{(s_1-s_2)^2+s_3^2} - (s_1-2s_2)}{\left(e^{\pm\sqrt{(s_1-s_2)^2+s_3^2}\left(\frac{\alpha}{2(cv-dv^2-b)}\xi-\xi_0\right)} - \dfrac{s_1-2s_2}{\sqrt{(s_1-s_2)^2+s_3^2}}\right)^2 - 1}, \tag{39}$$

where $s_1,\ s_2$ and s_3 are real constants.

Case 7: $D_2 > 0,\ D_3 > 0,\ D_4 > 0$, then $F(q) = (q-s_1)(q-s_2)(q-s_3)(q-s_4)$, snoidal wave solutions [13] come out as

$$q_9 = \frac{s_2(s_1-s_4)sn^2\left(\frac{\sqrt{(s_1-s_3)(s_2-s_4)}}{2}\left(\frac{\alpha}{2(cv-dv^2-b)}\xi-\xi_0\right),\ m\right)-s_1(s_2-s_4)}{(s_1-s_4)sn^2\left(\frac{\sqrt{(s_1-s_3)(s_2-s_4)}}{2}\left(\frac{\alpha}{2(cv-dv^2-b)}\xi-\xi_0\right),\ m\right)-(s_2-s_4)}, \tag{40}$$

$$q_{10} = \frac{s_4(s_2-s_3)sn^2\left(\frac{\sqrt{(s_1-s_3)(s_2-s_4)}}{2}\left(\frac{\alpha}{2(cv-dv^2-b)}\xi-\xi_0\right),\ m\right)-s_3(s_2-s_4)}{(s_2-s_3)sn^2\left(\frac{\sqrt{(s_1-s_3)(s_2-s_4)}}{2}\left(\frac{\alpha}{2(cv-dv^2-b)}\xi-\xi_0\right),\ m\right)-(s_2-s_4)}, \tag{41}$$

where $s_1,\ s_2,\ s_3$ and s_4 are real constants, and $m^2 = \frac{(s_1-s_4)(s_2-s_3)}{(s_1-s_3)(s_2-s_4)}$.

Case 8: $D_4 < 0\ \&\ ((D_2 < 0\ \&\ D_3 < 0) \| (D_2 = 0\ \&\ D_3 \le 0) \| D_2 > 0)$, then $F(q) = (q-s_1)(q-s_2)[(q-s_3)^2 + s_4^2]$, a cnoidal wave solution [13] comes out as

$$q_{11} = \frac{\varepsilon_1 cn^2\left(\frac{\sqrt{-2s_4o_1(s_1-s_2)}}{2o_1o}\left(\frac{\alpha}{2(cv-dv^2-b)}\xi-\xi_0\right),\ o\right)+\varepsilon_2}{\varepsilon_3 cn^2\left(\frac{\sqrt{-2s_4o_1(s_1-s_2)}}{2o_1o}\left(\frac{\alpha}{2(cv-dv^2-b)}\xi-\xi_0\right),\ o\right)+\varepsilon_4}, \tag{42}$$

where $s_1,\ s_2,\ s_3$ and s_4 are real constants, and

$$\begin{aligned}
\varepsilon_1 &= \frac{1}{2}(s_1+s_2)\varepsilon_3 - \frac{1}{2}(s_1-s_2)\varepsilon_4,\\
\varepsilon_2 &= \frac{1}{2}(s_1+s_2)\varepsilon_4 - \frac{1}{2}(s_1-s_2)\varepsilon_3,\\
\varepsilon_3 &= s_1 - s_3 - \frac{s_4}{o_1},\\
\varepsilon_4 &= s_1 - s_3 - s_4o_1,\\
E &= \frac{s_4^2+(s_1-s_3)(s_2-s_3)}{s_4(s_1-s_2)},\\
o_1 &= E \pm \sqrt{E^2+1}, \quad o^2 = \frac{1}{1+o_1^2}.
\end{aligned} \tag{43}$$

Case 9: $D_4 > 0$ & $((D_2 > 0 \ \& \ D_3 \leq 0) \| D_2 \leq 0)$, then $F(q) = [(q-s_1)^2 + s_2^2][(q-s_3)^2 + s_4^2]$, a straddled cnoidal-snoidal wave solution [13] comes out as

$$q_{12} = \frac{\begin{array}{l} \varepsilon_1 \operatorname{sn}\left(\frac{s_2\sqrt{\left(\varepsilon_3^2+\varepsilon_4^2\right)\left(o_1^2\varepsilon_3^2+\varepsilon_4^2\right)}}{\varepsilon_3^2+\varepsilon_4^2}\left(\frac{\alpha}{2\left(cv-dv^2-b\right)}\xi-\xi_0\right), o\right) \\ +\varepsilon_2 cn\left(\frac{s_2\sqrt{\left(\varepsilon_3^2+\varepsilon_4^2\right)\left(o_1^2\varepsilon_3^2+\varepsilon_4^2\right)}}{\varepsilon_3^2+\varepsilon_4^2}\left(\frac{\alpha}{2\left(cv-dv^2-b\right)}\xi-\xi_0\right), o\right) \end{array}}{\begin{array}{l} \varepsilon_3 \operatorname{sn}\left(\frac{s_2\sqrt{\left(\varepsilon_3^2+\varepsilon_4^2\right)\left(o_1^2\varepsilon_3^2+\varepsilon_4^2\right)}}{\varepsilon_3^2+\varepsilon_4^2}\left(\frac{\alpha}{2\left(cv-dv^2-b\right)}\xi-\xi_0\right), o\right) \\ +\varepsilon_4 \operatorname{sn}\left(\frac{s_2\sqrt{\left(\varepsilon_3^2+\varepsilon_4^2\right)\left(o_1^2\varepsilon_3^2+\varepsilon_4^2\right)}}{\varepsilon_3^2+\varepsilon_4^2}\left(\frac{\alpha}{2\left(cv-dv^2-b\right)}\xi-\xi_0\right), o\right) \end{array}}, \tag{44}$$

where s_1, s_2, s_3 and s_4 are real constants, and

$$\begin{aligned} \varepsilon_1 &= s_1\varepsilon_3 + s_2\varepsilon_4, \\ \varepsilon_2 &= s_1\varepsilon_4 - s_2\varepsilon_3, \\ \varepsilon_3 &= -s_2 - \frac{s_4}{o_1}, \\ \varepsilon_4 &= s_1 - s_3, \\ E &= \frac{(s_1-s_3)^2 + s_2^2 + s_4^2}{2s_2s_4}, \\ o_1 &= E + \sqrt{E^2-1}, \\ o &= \sqrt{\frac{o_1^2-1}{o_1^2}}. \end{aligned} \tag{45}$$

5. Results and discussion

We analyze the solitary wave and shock wave solutions as depicted in Figures 1 and 2. Each figure illustrates the effect of the full nonlinearity variable n on the wave dynamics, with surface plots, contour plots, and 2D plots providing detailed insights into the behavior of the solutions. The parameters are addressed constant across all figures as $v = 1.3$, $k = 2.2$, $a = 1.7$, $c = 0.6$, $d = 1.4$, $b = 3.2$, $\alpha = 2.4$, $s_2 = 1.8$, $s_1 = 0.6$ and $\xi_0 = 1$.

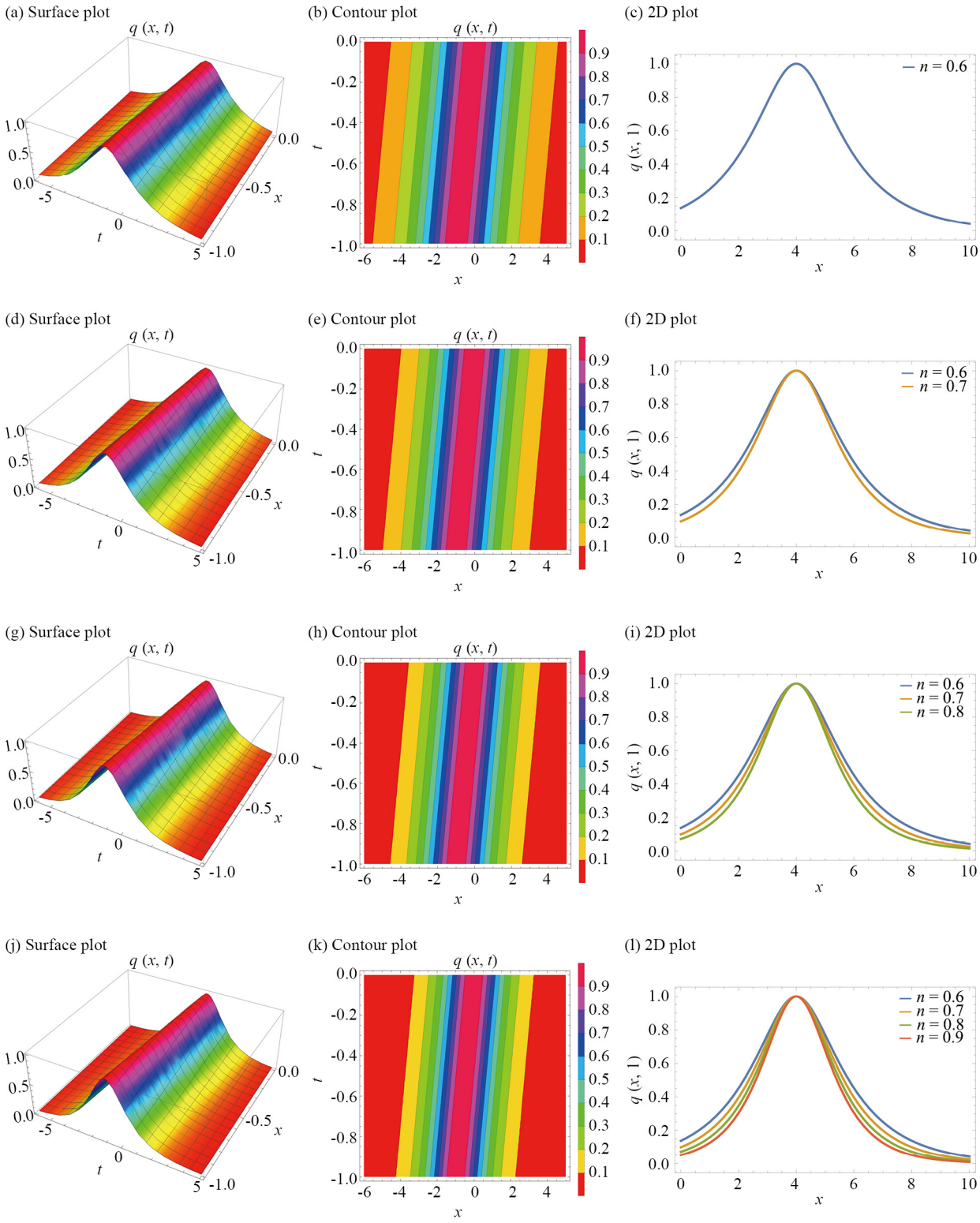
(a) Surface plot
q (x, t)
(b) Contour plot
q (x, t)
(c) 2D plot
n = 0.6
(d) Surface plot
q (x, t)
(e) Contour plot
q (x, t)
(f) 2D plot
n = 0.6
n = 0.7
(g) Surface plot
q (x, t)
(h) Contour plot
q (x, t)
(i) 2D plot
n = 0.6
n = 0.7
n = 0.8
(j) Surface plot
q (x, t)
(k) Contour plot
q (x, t)
(l) 2D plot
n = 0.6
n = 0.7
n = 0.8
n = 0.9
x
t
q (x, 1)

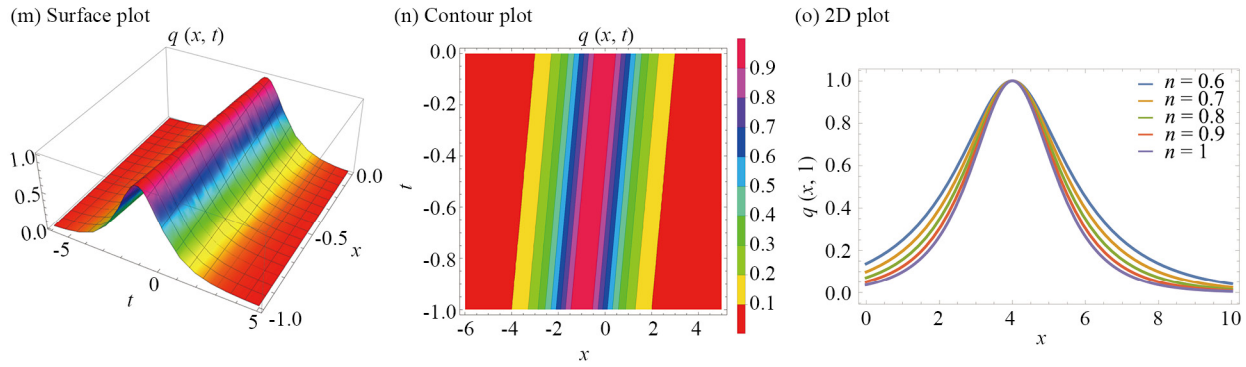

Figure 1. Exploring the features of a solitary wave

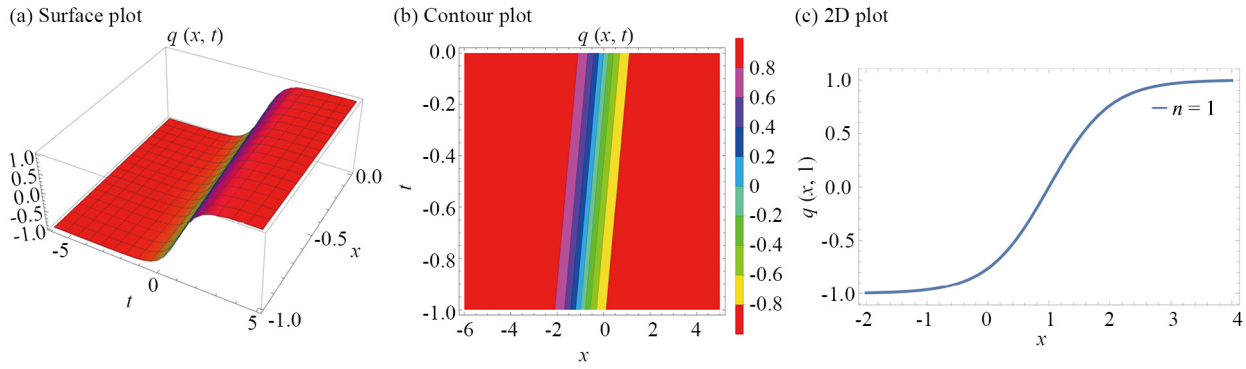

Figure 2. Exploring the features of a solitary wave

Figure 1 examines the solitary wave solution $q(x, t)$ described by solution (6), with fifteen subfigures depicting the effect of varying the full nonlinearity variable n across different visualization formats (surface, contour, and 2D plots). The detailed breakdown for each set of subfigures is as follows: Figures 1a, 1b, and 1c show the solitary wave dynamics for $n = 0.6$. In surface plot (1a), the solitary wave exhibits a localized peak with symmetric structure along the spatial and temporal axes, indicating the stability of the solution. The peak amplitude reaches its maximum at the center of the temporal domain and gradually decreases toward the edges. The contour plot (1b) confirms the solitary nature of the wave, with concentric contour lines around the peak. The symmetry is consistent with the surface plot, and the gradient in the spatial-temporal domain shows that the wave maintains its shape as it propagates. The 2D plot (1c) captures a cross-sectional view of the wave at a fixed time, revealing a sharp peak followed by a smooth decline in amplitude. The 2D view complements the 3D visualization by highlighting the precise profile of the solitary wave. Figures 1d, 1e, and 1f illustrate the solitary wave dynamics for $n = 0.7$. In surface plot (1d), as n increases, the wave profile becomes slightly more elongated in both time and space, though the overall solitary structure is preserved. The amplitude appears more concentrated, reflecting a steeper decay at the edges. In contour plot (1e), the contour density increases near the wave peak, indicating stronger nonlinearity effects. This suggests that as n increases, the solitary wave becomes more localized and sharper. In 2D plot (1f), the cross-sectional view again confirms the sharper and more localized nature of the wave as n increases, with the peak amplitude slightly higher than in the case of $n = 0.6$. Figures 1g, 1h, and 1i correspond to $n = 0.8$. In surface plot (1g), with further increase in n, the solitary wave becomes even more confined spatially, and the temporal evolution shows a pronounced peak. The amplitude rises faster and decays more rapidly at the boundaries. In contour plot (1h), the increased concentration of contour lines around the wave peak is evident, reflecting stronger nonlinear effects.

The contours are tightly spaced, indicating a sharp change in the amplitude around the center of the wave. In 2D plot (1i), the 2D cross-section continues to show a narrow, sharp peak, emphasizing the role of nonlinearity in concentrating the energy of the wave into a smaller spatial and temporal region. Figures 1j, 1k, and 1l show the results for $n = 0.9$. In surface plot (1j), the solitary wave becomes highly localized, with a steep rise in amplitude and rapid decay. The temporal profile shows a marked increase in the peak amplitude as the full nonlinearity variable approaches 1. In contour plot (1k), the contour plot reveals even tighter spacing around the peak, reinforcing the localization effect. The gradients in both space and time indicate that the wave is more sensitive to small changes in these parameters as n increases. In 2D plot (1l), the narrow and tall profile of the wave is evident, showcasing the significant impact of higher nonlinearity. The sharpness of the peak suggests that the solitary wave becomes increasingly confined, potentially enhancing its robustness against external perturbations. Figures 1m, 1n, and 1o represent the case of $n = 1$, the maximum value of the nonlinearity variable considered. In surface plot (1m), the wave exhibits the sharpest and most localized peak, with a steep drop-off in amplitude. The full nonlinearity leads to a more focused wave that retains its energy over a smaller region. In contour plot (1n), the contour lines are densely packed near the wave peak, illustrating the concentrated nature of the solitary wave. The rapid change in amplitude is particularly pronounced in this case. In 2D plot (1o), the 2D cross-section highlights the extreme localization of the wave, with a very high amplitude at the center and steep declines on either side. This suggests that the solitary wave solution becomes increasingly resilient as n approaches 1.

Figure 2 focuses on the shock wave solution $q(x, t)$ described by solution (35), with three subfigures that explore the effect of the full nonlinearity variable $n = 1$. In Figure 2a, the surface plot shows the development of a shock wave with a sharp discontinuity. The steep gradient in the amplitude across both space and time domains is characteristic of shock wave formation, where the wavefront propagates with a rapid rise in amplitude followed by a sharp drop-off. In Figure 2b, the contour plot confirms the presence of a shock wave, with tightly packed contour lines at the wavefront and a more gradual spacing behind it. The sharp transition between high and low amplitudes is clearly visible, indicating the non-smooth nature of the solution. In Figure 2c, the 2D plot provides a detailed view of the shock profile at a fixed time, displaying the characteristic abrupt change in amplitude. This profile underscores the fundamental difference between solitary and shock waves, with the latter exhibiting a discontinuous structure that arises from the nonlinear effects.

In summary, Figures 1 and 2 reveal the influence of the full nonlinearity variable n on both solitary and shock wave solutions. For solitary waves, as n increases, the wave becomes more localized and sharp, with higher amplitudes and steeper decay at the boundaries. The shock wave, on the other hand, demonstrates a rapid rise and fall in amplitude, with the formation of a distinct discontinuity. These results underscore the crucial role of nonlinearity in shaping the wave dynamics, with higher values of n leading to more pronounced effects in both solitary and shock wave solutions.

6. Conclusions

The current paper recovered and presented a wide range of results for the newly proposed model to study shallow water waves, namely the Boussinesq equation with cubic and generalized cubic form of nonlinearity. The generalized cubic nonlinear form was integrated using the traveling wave hypothesis while the cubic form of nonlinearity was taken up with the complete discriminant approach. The traveling wave hypothesis yielded solitary wave solution while the later gave way to a wide range of solutions. These are shock waves, singular solitary waves, plane waves, periodic solutions and cnoidal waves. Thus a full spectrum of solutions were recovered for the model using this couple of approaches. Singular solitary waves do not have any physical significance, as they do not correspond to any realizable or stable waveforms. In contrast, solitary waves, exhibit stable and physically meaningful behavior. Solitary waves, which are localized and maintain their shape over time, have well-established stability properties. Their persistence in a nonlinear medium highlights their physical relevance, unlike the singular solutions which lack such stability and meaningful representation in real-world scenarios. The multiplier approach retrieved the conservation laws and the corresponding conserved quantities are computed and presented.

The future prospect of the model stands on a very strong footing. The model will be extended with the perturbation terms that will bring the study closer to realistic situation. Additional integration schemes will be implemented to address

the extended model such as Lie symmetry and others [14–16]. The model is yet to be studied for two-layered as well as multi-layered shallow water flow, in which case vector coupled versions of the model will be established. Such studies are under way and the outcomes of these studies will be communicated as soon as they are finalized.

Acknowledgment

This work for the fifth author (AB) was funded by the budget of Grambling State University for the Endowed Chair of Mathematics. AB also thankfully acknowledges the financial support received from Universal Wiser Publisher Private Limited.

Conflict of interest

The authors declare no competing financial interest.

References

[1] Adamashvili GT. Two-component nonlinear wave of the cubic Boussinesq-type equation. *Physics Letters A*. 2023; 475: 128866. Available from: https://doi.org/10.1016/j.physleta.2023.128866.

[2] Biswas A, Vega-Guzman J, Bansal A, Kara AH, Aphane M, Yildirim Y, et al. Solitary waves, shock waves and conservation laws with the surface tension effect in the Boussinesq equation. *Proceedings of the Estonian Academy of Sciences*. 2023; 72(1): 17-29. Available from: https://doi.org/10.3176/proc.2023.1.03.

[3] Liu CS. Applications of complete discrimination system for polynomial for classifications of traveling wave solutions to nonlinear differential equations. *Communications in Computational Physics*. 2010; 181(2): 317-324. Available from: https://doi.org/10.1016/j.cpc.2009.10.006.

[4] Liu CS. Travelling wave solutions of triple sine-Gordon equation. *Chinese Physics Letters*. 2004; 21(12): 2369-2371. Available from: https://doi.org/10.1088/0256-307X/21/12/014.

[5] Wazwaz AM. The variational iteration method for rational solutions for KdV, $K(2, 2)$, Burgers, and cubic Boussinesq equations. *Journal of Computational and Applied Mathematics*. 2007; 207(1): 18-23. Available from: https://doi.org/10.1016/j.cam.2006.07.010.

[6] Malomed BA. New findings for the old problem: Exact solutions for domain walls in coupled real Ginzburg-Landau equations. *Physics Letters A*. 2022; 422: 127802. Available from: https://doi.org/10.1016/j.physleta.2021.127802.

[7] He S, Malomed BA, Mihalache D, Peng X, He Y, Deng D. Propagation dynamics of radially polarized symmetric Airy beams in the fractional Schrödinger equation. *Physics Letters A*. 2021; 404: 127403. Available from: https://doi.org/10.1016/j.physleta.2021.127403.

[8] Qiu Y, Malomed BA, Mihalache D, Zhu X, Peng J, He Y. Generation of stable multi-vortex clusters in a dissipative medium with anti-cubic nonlinearity. *Physics Letters A*. 2019; 383(22): 2579-2583. Available from: https://doi.org/10.1016/j.physleta.2019.05.022.

[9] Malomed BA. Multidimensional dissipative solitons and solitary vortices. *Chaos, Solitons and Fractals*. 2022; 163: 112526. Available from: https://doi.org/10.1016/j.chaos.2022.112526.

[10] Susanto H, Malomed BA. Embedded solitons in second-harmonic-generating lattices. *Chaos, Solitons and Fractals*. 2021; 142: 110534. Available from: https://doi.org/10.1016/j.chaos.2020.110534.

[11] He S, Malomed BA, Mihalache D, Peng X, Yu X, He Y, et al. Propagation dynamics of abruptly autofocusing circular Airy Gaussian vortex beams in the fractional Schrödinger equation. *Chaos, Solitons and Fractals*. 2021; 142: 110470. Available from: https://doi.org/10.1016/j.chaos.2020.110470.

[12] He S, Zhou K, Malomed BA, Mihalache D, Zhang L, Tu J, et al. Airy-Gaussian vortex beams in the fractional nonlinear-Schrödinger medium. *Journal of the Optical Society of America B*. 2021; 38(11): 3230-3236. Available from: https://doi.org/10.1364/JOSAB.438240.

[13] Drazin PG, Johnson RS. *Solitons: An Introduction*. 2nd ed. UK: Cambridge University Press; 1989.

[14] Chen M, Wang Z. Analytical three-periodic solution and interaction for nonlocal Boussinesq equation. *The European Physical Journal Plus*. 2023; 138: 893. Available from: https://doi.org/10.1140/epjp/s13360-023-04518-9.

[15] Hossain MD, Alam MK, Akbar MA. Abundant wave solutions of the Boussinesq equation and the $(2+1)$-dimensional extended shallow water wave equation. *Ocean Engineering*. 2018; 165: 69-76. Available from: https://doi.org/10.1016/j.oceaneng.2018.07.025.

[16] Liang YH, Wang KJ. Bifurcation analysis, chaotic phenomena, variational principle, hamiltonian, solitary and periodic wave solutions of the fractional benjamin ono equation. *Fractals*. 2025; 33(01): 1-13. Available from: https://doi.org/10.1142/S0218348X25500161.